

## Geochemical Monitoring of the Seismic Activities and Noble Gas Characterization of the Geothermal Fields along the Eastern Segment of the Büyükk Menderes Graben

Selin Süer<sup>1</sup>, Thomas Wiersberg<sup>2</sup>, Nilgün Güleç<sup>3</sup>, Jörg Erzinger<sup>2</sup> and Mahmut Parlaktuna<sup>4</sup>

<sup>1</sup>General Directorate of Mineral Research and Exploration, Eskişehir yolu, 06520 Ankara, Turkey

ssuer@metu.edu.tr, selsuer@gmail.com

<sup>2</sup>Deutsches GeoForschungsZentrum, Telegrafenberg, 14473 Potsdam, Germany

wiers@gfz-potsdam.de, erz@gfz-potsdam.de

<sup>3</sup>Middle East Technical University, Department of Geological Engineering, 06531 Ankara, Turkey

nilgun@metu.edu.tr

<sup>4</sup>Middle East Technical University, Department of Petroleum and Natural Gas Engineering, 06531 Ankara, Turkey

mahmut@metu.edu.tr

**Keywords:** Continuous Geochemical Monitoring, Seismicity, Geothermal Water, Isotopes, Gases

### ABSTRACT

Continuous monitoring of geochemical parameters related to gases in geothermal fields is widely used in seismically active regions of the crust. In this respect, a real time gas monitoring setup was installed near a bubbling pool in the Tekke Hamam geothermal field located along the eastern end of the Büyükk Menderes Graben in Western Anatolia, Turkey. This site was chosen because it experiences frequent low-magnitude seismic activities. In this field, the discharged gas was collected with a funnel at the bottom of a pool and piped into a mass spectrometer for on-line analysis of CO<sub>2</sub>, CH<sub>4</sub>, H<sub>2</sub>, N<sub>2</sub>, H<sub>2</sub>S, O<sub>2</sub>, He and Ar. In addition to online monitoring, gas and water samples were collected from the Tekke Hamam and Kızıldere geothermal fields, the latter being also located along the eastern segment of the Büyükk Menderes Graben, 4 km northeast of Tekke Hamam. During continuous monitoring from November 2007 to October 2008, significant variations were detected in the gas compositions of the bubbling pools. These variations were evaluated on a monthly basis and are being correlated with both seismic and meteorological data compiled during the course of monitoring. In addition to the gas monitoring data, a general geochemical characterization of the Kızıldere and Tekke Hamam geothermal fields is being performed on the basis of isotope analyses of both water and gas samples collected from the geothermal fields.

### 1. INTRODUCTION

Since the 1960s, geochemical monitoring studies have become increasingly popular for the prediction of earthquakes. Studies performed in this respect have mostly focused on the utilization of either periodical or real-time/continuous monitoring techniques for understanding both the mechanisms inducing earthquakes and the associated response in the affected region of the crust (Thomas, 1988; Toutain and Baubron, 1999).

Changes in the chemical composition of the ascending fluids are linked to seismic activities and can be viewed as earthquake precursors provided that the mechanisms are well understood. In this respect, water and gaseous species have been increasingly monitored with particular focus on

gases, which have proved to be more sensitive tracers of seismically induced variations.

The mobility of gases makes them perfect tracers in earthquake prediction studies. Considerable variations in dissolved gases in natural waters have been reported before, during, and after seismic activities and are considered to reflect physical and chemical processes occurring at depth, such as fluid-mixing, micro-fracture formation and permeability modifications (Hirabayashi and Kusakabe, 1985). Amongst the gases of interest, the most responsive and sensitive ones are the noble gases (He, Ne, Ar, Kr, Xe, with particular focus on the <sup>3</sup>He/<sup>4</sup>He-ratio). The concentrations and isotopic compositions of these gases have recently been used as natural tracers in the investigation of the origin of geothermal fluids, the study of reservoir processes and the monitoring of seismicity (Lupton, 1983; King, 1986; Thomas, 1988; Kennedy and Truesdell, 1996; Kipfer et al., 2002; Lippmann et al., 2003, Lippmann et al., 2005; Wiersberg and Erzinger, 2007). Changes in gas compositions such as CO<sub>2</sub>, H<sub>2</sub>S, CH<sub>4</sub>, and H<sub>2</sub> and variations in He/Ar, CH<sub>4</sub>/Ar, N<sub>2</sub>/Ar, and <sup>3</sup>He/<sup>4</sup>He ratios have also been proposed to be potential precursors of seismic activities (Sugisaki, 1978; Kawabe, 1985; Sano et al., 1998; Italiano and Martinelli, 2001).

The present study is directed at the geochemical monitoring of seismicity via gas geochemistry of the hydrothermal fluids along the eastern end of the Büyükk Menderes Graben, which encompasses the highest enthalpy geothermal fields in Turkey. The locations of the Tekke Hamam and Kızıldere geothermal fields are shown in relation to a tectonic map of Turkey in Figure 1. The study is focused on two major aspects: i) the continuous monitoring of gas compositions of a bubbling pool in Tekke Hamam geothermal field and ii) the hydrogeochemical characterization of the Tekke Hamam and the nearby Kızıldere geothermal fields. Of the two geothermal fields, Kızıldere geothermal field is located on the northern boundary fault, whereas Tekke Hamam is located on the southern boundary fault in the Büyükk Menderes Graben. The results obtained so far from an on-going research project that started in 2006 are presented here.

## 2. TECTONIC SETTING AND RECENT SEISMICITY

The geothermal fields concerned in this study are located within the Western Anatolian Graben System (WAGS) (shown in Figure 1). The WAGS comprises one of the major structural zones in Turkey that developed during the neotectonic period in response to the intracontinental convergence following the Late Miocene collision of the Arabian promontory with Eurasia (McKenzie, 1972; Dewey and Şengör, 1979).

The Western Anatolian Graben System is an area of intense seismic activity which is related to the east-west trending graben complexes in the Aegean region. The broad tectonic framework of the Aegean is dominated by the rapid westward motion of the Anatolian Plate relative to the Black Sea plate and west-southwestward motion relative to the African Plate (McKenzie, 1972). Fault plane solutions and maps of surface breaks suggest that motion is to the west on a number of E-W grabens. The westward movement of Turkish plate carries western Turkey through an extensional zone where the continent is stretched and its thickness halved. According to Dewey and Şengör (1979), the tectonics of the Aegean region involves complex slip patterns across the boundaries of several microplates that segment the end of the Anatolian Plate. The westward escape is facilitated by the subduction of the oceanic floor of the eastern Mediterranean at the Hellenic trench. Although the westward motion is accomplished simply at the Hellenic trench and along the East and North Anatolian transform faults, the motion is retarded by intracontinental locking between the Sea of Marmara and the northern end of the Hellenic trench. This locking results in a complex pattern of grabens and thrust and strikeslip deformations that segment the western end of the Anatolian plate and the southwestern corner of the Black Sea plate into a number of small scholles. According to the ages obtained from geophysical evidence and based on the initiation of subduction along Hellenic Trench, the timing of initiation of extension in Western Anatolia appears to span a range

from 12 Ma (Le Pichon and Angelier, 1979) to 26 Ma (Spakman, 1989).

The *Büyük Menderes Graben*, which is one of the major grabens characterizing the WAGS, encompasses the *Kızıldere* and *Tekke Hamam* geothermal fields located on the northern and southern boundary faults of the graben, respectively (shown in Figure 1). The region is dominated by low-magnitude seismic swarms (generally  $3.0 < M < 4.0$ ), which are especially concentrated along the Çameli-Denizli district in close vicinity to the geothermal fields of interest. No major destructive seismic event, exceeding  $M: 5.0$  occurred in the area during the course of monitoring from November 2007 to October 2008.

## 3. REGIONAL GEOLOGY AND HYDROGEOLOGIC OUTLINE

The basement of the geothermal fields is represented by the Menderes Massif metamorphics (shown in Figure 1). The Menderes Massif metamorphics are comprised, from bottom to top, of gneisses, schists, and an alternation of quartzites, micaschists and marbles (İğdecik formation) (Şimşek, 1985). The Neogene sedimentary rocks that lie above the metamorphics are represented, from bottom to top, by the *Kızılburun* formation which consists of conglomerate and sandstone; the *Sazak* formation, which consists of limestone and marl; and the *Kolonkaya* formation, consisting of marl and sandstone (Şimşek, 1985). The Upper Pliocene aged *Tosunlar* formation lying above all these units is represented by poorly consolidated conglomerates, sandstone and mudstone. The Quaternary deposits unconformably overlie all the units and are represented by alluvium, terrace deposits, slope debris and travertine (Şimşek, 1985). Western Anatolia is also characterized by widespread magmatic activity prevailing in the region since the Paleozoic. The products of this magmatic activity are granitic intrusions of Paleozoic to Tertiary age and the Tertiary to recent volcanics covering extensive areas.

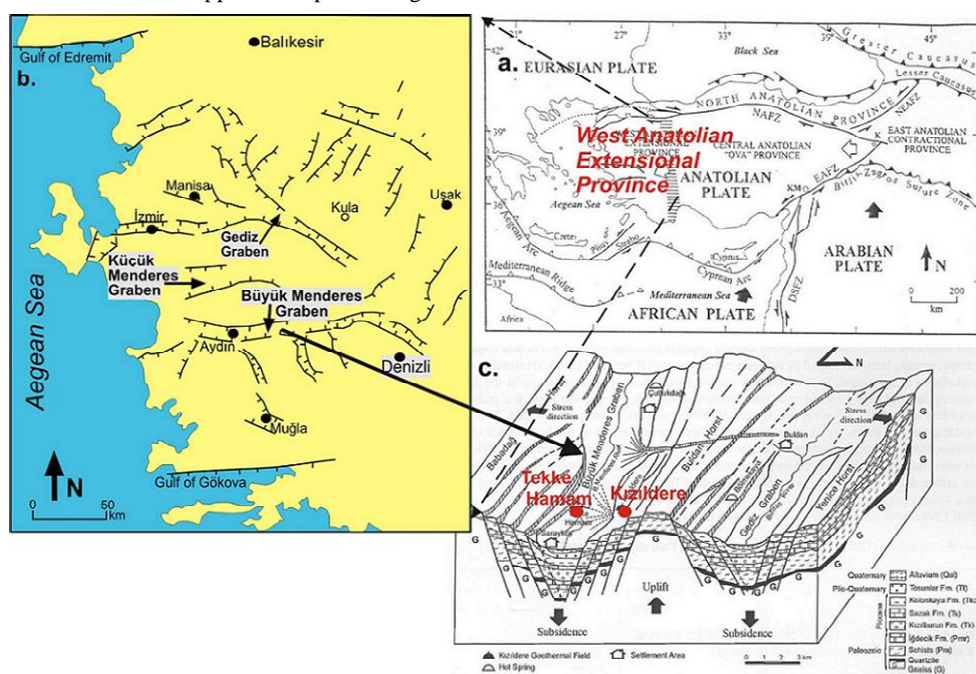


**Figure 1.** a). Tectonic map of Turkey (Bozkurt, 2001), b). Major structural elements of Western Anatolia (Bozkurt, 2001), c). Location of Kızıldere and Tekke Hamam geothermal fields in the *Büyük Menderes Graben* (Şimşek, 1985).

The Kızıldere geothermal field is characterized by several hot springs and steam vents having temperatures between 36 and 100°C. Hot waters generally issue from the major east-west trending faults, or from the intersection of the east-west trending faults with faults of differing trends. However, due to the drilling activities in the field, especially hot springs have dried out significantly. In the Tekke Hamam geothermal field, on the other hand, there are a number of hot water springs and mud pools that exhibit gas emissions. The temperatures of these waters are between 57 and 99 °C and their total discharge is about 30 l/s.

There are two main reservoirs in the field. The limestone unit of the Pliocene Sazak Formation forms the first and topmost reservoir. The marble-quartzite-schist alternation in the İğdecik formation forms the second and lower reservoir in the field. There is also the possibility of a third reservoir in the field, which is a gneiss-quartzite unit (Şimşek, 1984). The Kızılburun, Kolonkaya and Sazak formations of the Pliocene units constitute the cap rock of the geothermal system.

#### 4. METHODS OF STUDY

This study was realized through two major steps: i) real-time gas monitoring in Tekke Hamam geothermal field and ii) geochemical characterization of Kızıldere and Tekke Hamam geothermal fields.

##### 4.1 Sampling and Analyses

Two major sampling campaigns were conducted in the Tekke Hamam and Kızıldere geothermal fields: the first lasted from November 19–26, 2007, and the second lasted from August 30–September 2, 2008. For the geochemical characterization studies, gas and water samples were collected from both the Kızıldere and Tekke Hamam geothermal fields.

The sampling localities in Tekke Hamam include bubbling pools (Pools 1, 2, 3, 4, 5, 6), a drilling well (Umut-1), 2 hot water tanks near the drilling well (TH-6, TH-7), a hot spring (TH-8) and a cold spring (TH-cold). Gas samples were taken from the bubbling pools, whereas the water samples were taken from all sample sites. In Kızıldere, a total of 8 hot water wells (KD-6, KD-13, KD-14, KD-15, KD-16, KD-21, KD-22, and R-1) were sampled for water analyses. Gas samples, on the other hand, could be taken from all wells except for R-1.

For anion, cation-trace element and stable isotope ratio ( $^{18}\text{O}/^{16}\text{O}$  and D/H) analyses, water samples were collected via filtering into three sets of 100 ml high density polyethylene bottles, separately. For the noble gas analyses, gases were collected in annealed copper tubes, which were sealed via clamps.

Cation-trace element and anion analyses were carried out at the ACME and SRC Laboratories for the first and second sampling campaigns, respectively.  $^{18}\text{O}/^{16}\text{O}$  and D/H analyses, on the other hand, were conducted at the laboratories of University of Waterloo. Finally, noble gas analyses were performed at the GFZ-Potsdam noble gas laboratory.

The physical parameters (T, pH, EC, DO, TDS) of the samples were measured by a multiparameter measurement device directly in the field for each sampling point. The sample types and the UTM coordinates of the sampling sites from Kızıldere and Tekke Hamam geothermal fields are presented in Table 1.

**Table 1. Sample types and UTM coordinates of the sampling sites**

Location	Sample Name	Sample Type	UTM		Altitude (m)
			E	N	
Tekke Hamam	Pool 1	Bubbling pool	660686	4198572	141
	Pool 2		660685	4198555	141
	Pool 3		660685	4198547	141
	Pool 4		660697	4198566	146
	Pool 5		660701	4198583	145
	Pool 6		660708	4198564	142
Kızıldere	Umut-1	Production Well	660751	4198608	138
	TH-6		660697	4198630	150
	TH-7		660704	4198556	132
	TH-8		660564	4198691	137
	TH-Cold		660564	4198691	137
	KD-13		661882	4202637	195
	KD-15		662170	4203002	202
	KD-16		662094	4202888	196
Kızıldere	KD-22	Production Well	661983	4202735	198
	KD-6		661906	4202419	175
	KD-14		662002	4202868	197
	R-1		661036	4201912	148
	KD-21		662172	4202781	200

#### 4.2 Monitoring Setup

During the construction stage of the online monitoring station, a plastic funnel was connected inversely to plastic tubing and was immersed into a bubbling pool (Pool 2) in Tekke Hamam. The gases were then introduced into the monitoring station via the plastic tubing connected to the inverted funnel inside the pool. A physical connection was maintained between the funnel, the Quadrupole Mass Spectrometer (QMS) and flowmeter inside the station. A temperature sensor was also inserted into the pool and was sealed with concrete together with the plastic tubing to avoid external disturbances.

After the construction of the gas line, electrical connections were established between the QMS, the flowmeter and a computer. A data logger was used to transfer the data recorded by the flowmeter and the temperature sensor to the computer. An uninterrupted power supply unit (UPS) was also connected to the system to avoid loss of power during power cut off for a few minutes before the generator functioned.

The QMS in the station was set to measure the Ar, CO<sub>2</sub>, CH<sub>4</sub>, H<sub>2</sub>, H<sub>2</sub>S, He, N<sub>2</sub> and O<sub>2</sub> gases continuously in one minute intervals (vol.%). The flowmeter and the data logger were set to measure the gas flow rate (l/min) and pool temperature (°C) at the same time interval as the mass spectrometer. After the calibration of the mass spectrometer with certain gas mixtures, the system was ready to continuously monitor the gases.

During the course of monitoring, the seismic events that occurred in close vicinity to the field were routinely compiled from the website records of the Kandilli Observatory and Earthquake Research Institute in Turkey. The daily meteorological data, including air temperature, air pressure and precipitation, were all obtained from the Turkish State Meteorological Service.

#### 5. CHEMICAL AND STABLE ISOTOPIC COMPOSITIONS

The hydrogeochemical facies of the samples collected during the second sampling campaign are presented in Figure 2 in a Piper diagram. As can be seen from the diagram, the water samples taken from the bubbling pools in Tekke Hamam showed similar anion compositions but slightly different cation compositions. Pools 2 and 3 are located inside the mixed water border in terms of cations, whereas for the other pool, Na samples appeared to be the dominant cation. Since SO<sub>4</sub> was the dominant anion for all

of the samples in Tekke Hamam, mainly two types of waters can be defined: Na-SO<sub>4</sub> type waters in Pools 1, 4, 5, 6 and well samples and Na-Ca-SO<sub>4</sub> type waters in Pools 2 and 3. The cold water sample, on the other hand, showed a Ca-Mg-SO<sub>4</sub> character. The SO<sub>4</sub> dominancy in Tekke Hamam waters possibly reflects the interaction with anhydrite and gypsum in the Neogene sedimentary sequence. It is also worth noting that, although the pool samples have low temperatures (mainly around 30°C-40°C), they are characterized by very high Total Dissolved Solid (TDS) levels, reaching up to nearly 10,000 mg/l in Pools 2 and 5.

The water samples taken from the wells in the Kızıldere geothermal field are all Na-HCO<sub>3</sub> type waters. These waters are also characterized by high SO<sub>4</sub> contents, probably controlled by the saturation with respect to anhydrite. The bicarbonate character of waters in Kızıldere seems to be compatible with the dissolution of the reservoir rocks that are dominated by limestone and marble-quartzite-schist alternations. Ion exchange with the overlying sediments, including impermeable clayey levels, is probably responsible for the dominance of Na cation in the hot waters.

The  $\delta^{18}\text{O}$  and  $\delta\text{D}$  values of waters from Kızıldere range between -6.25‰ and -4.23‰ and between -54.55‰ and -51.01‰, respectively. The Tekke Hamam waters have  $\delta^{18}\text{O}$  values ranging from -8.60‰ to 0.89‰ and  $\delta\text{D}$  values from -65.12‰ to -8.97‰.

In Figure 3, the isotope compositions of the waters are presented separately as  $\delta^{18}\text{O}$  vs.  $\delta\text{D}$  diagrams for the first and second sampling campaigns. The  $\delta^{18}\text{O}$  and  $\delta\text{D}$  compositions of the geothermal waters reveal an essentially meteoric origin for both Kızıldere and Tekke Hamam geothermal waters, with superimposed effects of evaporation and water-rock interaction. It can be readily seen in Figure 3 that, for the first sampling period, the pool

samples taken from Tekke Hamam lay along and/or close to the global meteoric water line (GMWL). The more negative isotope value of the well waters from Tekke Hamam points to the possibility that the water originates from an aquifer that is recharged from higher altitudes, as opposed to the pool waters. For the second sampling period, it was seen that the Tekke Hamam pool waters deviated from the GMWL and were aligned along an evaporation line. The different distribution of the pool waters for the two sampling periods is possibly related to the different seasonal conditions prevailing during the two sampling periods (the first during the rainy season, and the second during the dry and hot season), and most probably reflects the effects of intense evaporation processes during the hot season.

The Kızıldere well waters, on the other hand, generally lie to the right of the GMWL and reflect the effects of intense water-rock interaction processes under high temperature conditions. The Kızıldere waters show similar distributions for the two sampling periods and suggest that these waters are not affected by seasonal conditions.

## 6. HELIUM CONTENTS

The isotopic composition of He in the gas samples is given in Table 2 along with the He and Ne abundances. The  $^3\text{He}/^4\text{He}$  ratios range from 2.4 to 2.9 R<sub>a</sub> for Tekke Hamam gas samples, and from 1.1 to 2.1 R<sub>a</sub> for Kızıldere samples. The higher  $^3\text{He}/^4\text{He}$  ratios of the gases from Tekke Hamam bubbling pools suggest a relatively higher mantle-helium contribution for these samples than the samples from Kızıldere.

In the Kızıldere geothermal field, a SW-NE reaching trend toward lower R<sub>a</sub> values can be observed. Furthermore, the R<sub>a</sub> values roughly correlate with the well depths, showing higher R<sub>a</sub> values in deeper wells. One possible explanation is the mixing between a shallow fluid reservoir with a lower  $^3\text{He}/^4\text{He}$  ratio and a deeper reservoir with a higher one.

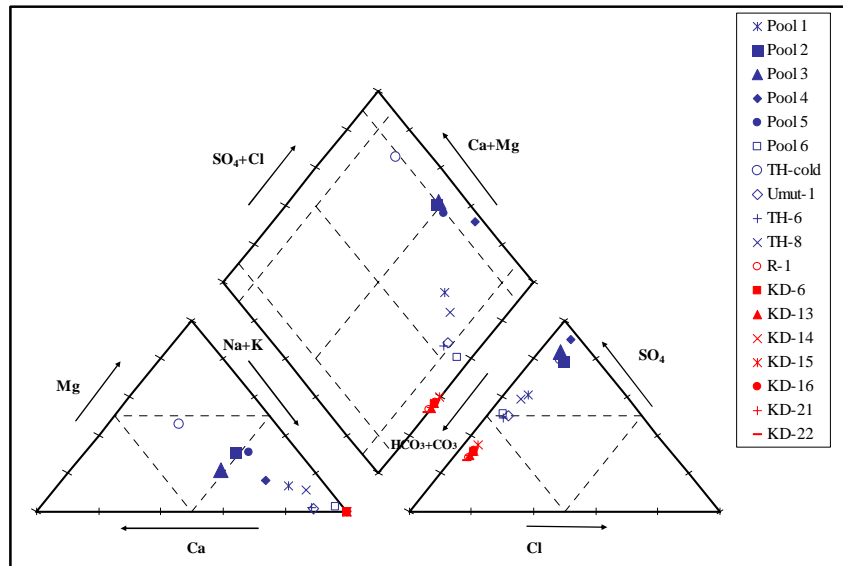
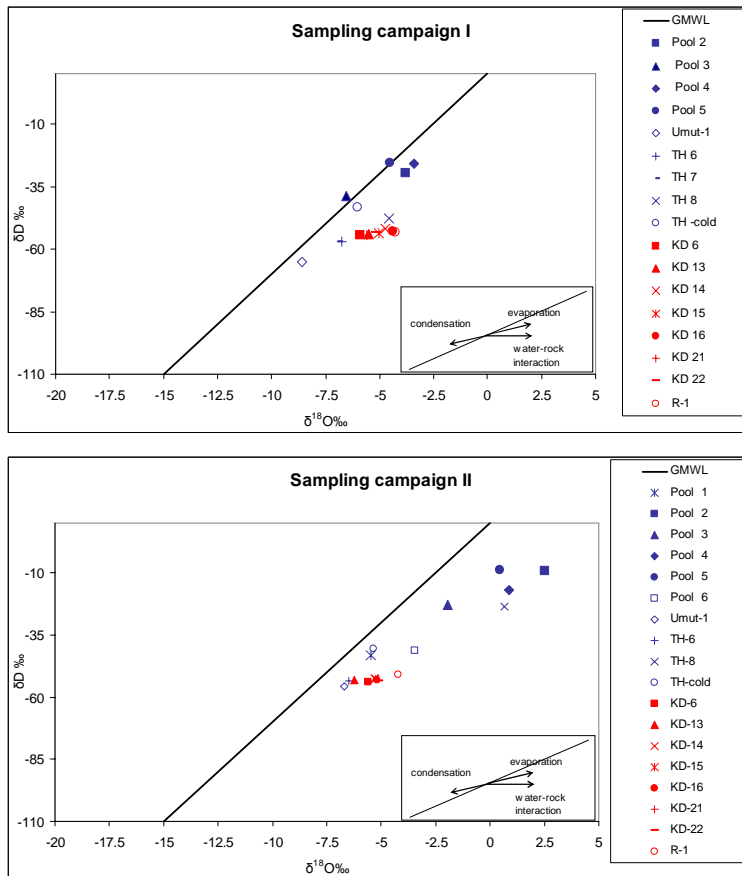


Figure 2. Piper diagram of the waters from Kızıldere and Tekke Hamam geothermal fields (Sampling Campaign II).



**Figure 3.**  $\delta^{18}\text{O}$  vs.  $\delta\text{D}$  diagram for Kızıldere and Tekke Hamam samples (GMWL: Global Meteoric Water Line from Craig (1961)).

**Table 2.** He isotope measurements on the gas samples from the geothermal fields

Sample	Location	Sampling Campaign	${}^4\text{He}$ [mbar]	${}^{20}\text{Ne}$ [ $10^{-3}$ mbar]	${}^3\text{He}/{}^4\text{He}$ [R/R <sub>earth</sub> ]
Pool 1	Tekke Hamam	I	0.001576	0.0403	2.790
Pool 2		I	0.00249	0.1964	2.573
Pool 3		II	0.00351	0.1308	2.359
Pool 3		I	0.00330	0.1246	2.740
Pool 4		I	0.001817	0.0947	2.863
Pool 5		I	0.00204	0.0952	2.780
KD_6	Kızıldere	I	0.001267	0.01745	2.050
KD_6		II	0.00222	1.200	1.793
KD_13		I	0.001466	0.371	1.705
KD_14		I	0.000492	0.0815	1.312
KD_15		I	0.00206	0.01043	1.178
KD_16		I	0.000479	0.0224	1.136
KD_21		II	0.000927	0.4485	1.490
KD_22		II	0.001129	0.1516	1.476

## 7. CONTINUOUS MONITORING

From the end of November 2007 until the end of October 2008, a real-time monitoring setup was operated near a bubbling pool in the Tekke Hamam geothermal field. During continuous monitoring, the QMS was set to measure  $\text{CO}_2$ ,  $\text{CH}_4$ ,  $\text{O}_2$ ,  $\text{H}_2\text{S}$ ,  $\text{H}_2$ ,  $\text{He}$ ,  $\text{Ar}$  and  $\text{N}_2$  simultaneously, at intervals of one minute. All gases were set to be measured by the Channel Electron Multiplier (CEM) detector. Meanwhile, the flow rate and the pool temperature were measured at the same time intervals by a flowmeter and a temperature sensor, respectively.

The major component of the bubbling gases coming from the pool was  $\text{CO}_2$ , with values around 96%. The second most abundant component in the gas mixture was  $\text{N}_2$ . Other components, in decreasing abundance, were  $\text{CH}_4$ ,  $\text{O}_2$ ,  $\text{H}_2\text{S}$ ,  $\text{Ar}$ ,  $\text{H}_2$  and  $\text{He}$ .

The high  $\text{CO}_2$  and low  $\text{O}_2$  values of the gases from the pool point to a deep origin of these gases. The low  $\text{O}_2$  and  $\text{N}_2$  values detected in the gas composition suggest the absence of air contamination.

### 7.1. Components of Variation

Different types of variation patterns have been identified from the temporal variation diagrams: daily variations, having a daily cyclic variation profile for each specific parameter; multi-day variations, lasting for more than 2 or 3 days; and finally, abnormal positive or negative peaks outside the profile of daily variation patterns.

#### 7.1.1 Daily and Multi-day variations

The real-time monitoring of gases revealed the existence of a daily variation pattern for all of the monitored parameters. The daily variation profile is characterized by daily variation amplitudes which differ for each specific parameter. The nearly 24 hour cycle of the daily variation profiles observed in the monitored parameters most probably depict tidal effects rather than meteorological effects. Tides can cause a daily cycle of compressive and tensile stress along faults. This can increase or decrease the permeability of faults and can control the migration of gases and/or liquids. Therefore, the daily cycles of tides in

the crust can result in daily cyclic trends observed in the gases.

The multi-day variations, on the other hand, were not strictly observed in every monitored parameter. Multi-day variation profiles generally last for 2 or 3 days and also shows the daily variation cycles. The reason for the multi-day variations is not yet resolved; however, since these variations also exceed the daily variation profile, they may be related to either meteorological or seismic events.

### 7.1.2 Geogenic Signals

Some distinct alterations beyond the daily variation profiles in the gas composition occurred on the recordings, which appeared to be independent of the changes observed in the meteorological parameters. These variations possibly indicate variations in the stress of a fault or fracture. Seismicity can trigger the opening of new or present pathways for ascending fluids and can therefore lead to an increase or decrease in the flow of gases from the depths, which in turn can appear as abnormal variations in the gas composition. In most cases, these abnormal variations, such as peaks (positive or negative), were accompanied by seismic activities occurring in the vicinity of the area. This coincidence indicates a possible relationship between the changes in the geochemical data and the seismic events occurring nearby. Since the area of interest in this study experienced several frequent low-magnitude seismic events, these variations are possibly related to the composite effect of the seismic events rather than the effect of a single event.

During monitoring, the seismic events with magnitude  $M < 3.0$  were not recorded in the geochemical data. In addition, there is not any record of a seismic event having a magnitude exceeding 5.0. While dealing with the presentation of seismic events in the temporal variation diagrams, a new parameter called Relative Seismicity was created and calculated by taking into account the magnitude, focal depth and epicentral distance between each seismic event and the bubbling pool from which the gases were monitored.

Around December 17, 2007, significant variations were recorded, as shown in Figure 4. On this date, a very rapid and sharp increase was detected in the gas flow rate, with values increasing from nearly 0.2 l/min to 0.35 l/min. The increase in the gas flow rate was also coupled with increases in  $O_2$ ,  $CH_4$ ,  $H_2S$ ,  $H_2$  and Ar. The observed increase lasted for nearly 2 days and later, the flowrates returned to their initial values. Since there was no significant variation in the meteorological parameters during this date, the variations detected can probably be correlated with the seismic activities that occurred in the area around December 17. The frequent nature of seismic activities in the vicinity of the fields leads to the consideration of the variations related to the composite effect of seismic activities instead of the effects of a single seismic event.

During the first week of June 2008, distinct variations were observed in some parameters of gas compositions ( $CO_2$ ,  $CH_4$ ,  $H_2S$ ) during the time period of June 4-8. These variations are plotted in Figure 5. A distinct decrease was also observed in the gas flow rate during the same time interval. The daily variation profile of  $CO_2$  was also slightly altered during this time period. Since there were no anomalous variations in the meteorological parameters, the recorded variations were correlated with the seismic activities that occurred in the area at that time.

In order to predict seismic activities, it is important to accumulate background gas composition data during relatively quiescent periods. The high frequency of seismic activities in the vicinity of Denizli makes it a difficult issue to determine the background values of the recorded gas compositions. Nevertheless, sudden variations in gas compositions and gas flow rates can be accepted as anomalies and can be correlated with the seismic activities occurring nearby. The anomalous variations can be interpreted as a possible consequence of the crustal permeability changes induced by seismicity. However, further statistical analysis should be performed in order to better evaluate the changes that occurred in relation to seismic events.

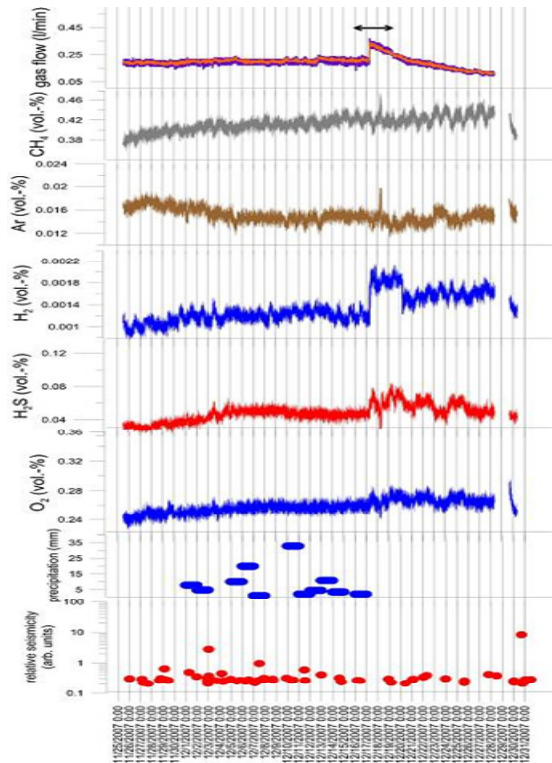


**Figure4. Temporal variation diagram for November-December 2007 period.**

### **7.2. Meteorological Effects**

Within the monitored parameters, the pool temperature seemed to be very sensitive to meteorological factors, especially air temperature. The variations in the daily average air temperature were generally directly proportional to the variations detected in the pool temperature. Parameters other than the pool temperature seem to be independent of meteorological processes and are more likely to reflect the effects of seismicity.

### **8. CONCLUSIONS**

1. The water samples from Kizildere and Tekke Hamam geothermal fields are dominantly  $Na-HCO_3$  and  $Na-SO_4$  in character, respectively. The cold water taken from Tekke Hamam is  $Ca-Mg-SO_4$  in character.
2. The oxygen- and hydrogen-isotope compositions point to a meteoric origin of the geothermal waters in both fields, with superimposed effects of evaporation and water-rock interaction.

3. The  ${}^3\text{He}/{}^4\text{He}$  ratios of Tekke Hamam waters are relatively higher than the Kızıldere waters and possibly point to a higher mantle-helium contribution.

4. Temporal variations examined so far reveal the existence of a daily cyclic profile for all of the monitored parameters, each having different amplitudes of variation. These daily cycles are possibly related to tidal effects. The variations exceeding the daily cyclic profile were mostly correlated with the seismic activities occurring in the vicinity of the field.

5. The pool temperature seemed to be the only parameter sensitive to meteorological effects. Other parameters appeared to be independent of the variations in meteorological processes. This can suggest that the gases coming from the pool originated at great depths.

6. For a more precise visualization of temporal variations in relation to seismic activities and meteorological factors, it is necessary to evaluate the monitored data set by using some statistical techniques, which will lead to a better understanding of the variation components.

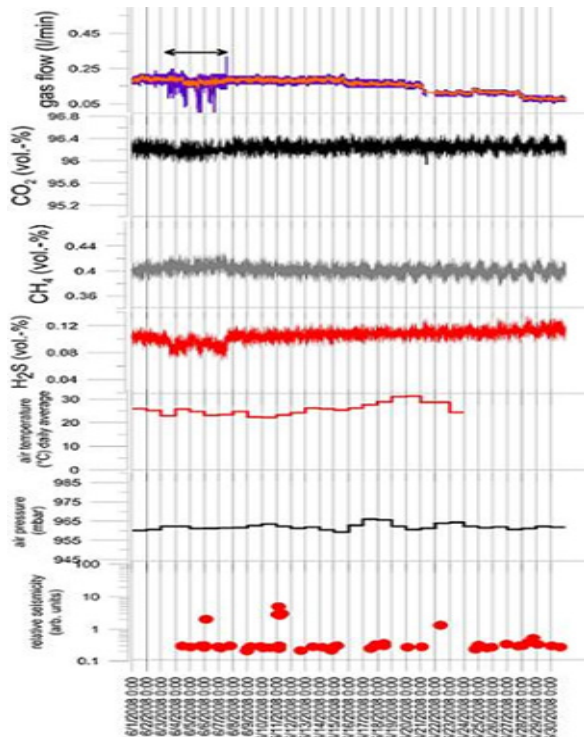


Figure 5. Temporal variation diagram for June 2008 period.

## 9. REFERENCES

Bozkurt, E.: Neotectonics of Turkey - a synthesis, *Geodinamica Acta*, **14**, (2001), 3-30.

Craig, H.: Isotopic Variations in Meteoric Waters, *Science*, **133**, (1961), 1702-1703.

Dewey, J.F., and Şengör, A.M.C.: Aegean Sea and Surrounding Regions: Complex Multiplate and Continuum Tectonics in a Convergent Zone, *Geol. Soc. Am. Bull Part I*, **90**, (1979), 84-92.

Hirabayashi, J., and Kusakabe, M.: A review on the Chemical Precursors of Volcanic Eruptions, *Bull. Volcanol. Soc. Jpn.* **30** (1985), 171-183.

Italiano, F., and Martinelli, G.: Anomalies of Mantle-derived Helium During the 1997-1998 Seismic Swarm of Umbria-Marche, Italy, *Geophysical Research Letters*, **28**, (2001), 839-842.

Kawabe, I.: Anomalous Changes of  $\text{CH}_4/\text{Ar}$  Ratio in Subsurface Gas Bubbles as Seismo-geochemical Precursors at Matsuyama, Japan, *Pure and Applied Geophysics*, **122**, (1984), 194-214.

Kennedy, B.M., and Truesdell, A.H.: The Northwest Geysers High-temperature Reservoir: Evidence for Active Magmatic Degassing and Implications for the Origin of The Geysers Geothermal Field, *Geothermics*, **25**, (1996), 365-387.

King, C.Y.: Gas Geochemistry Applied to Earthquake Prediction. An Overview, *JGR*, **91**, No. B12, 12, (1986), 269-281.

Kipfer, R., Aeschbach-Hertig, W., Peeters, F., and Stute, M.: Noble Gases in Lakes and Groundwaters, in Noble Gases in Geochemistry and Cosmochemistry, Rev. Mineral. Geochem., vol. 47, edited by D. Poercelli, C. Ballentine, and R. Wieler, pp. 615-700, Mineral Soc. Of America, Washington, D.C.

Le Pichon, X., and Angelier, J.: The Hellenic arc and Trench system: A Key to the Neotectonic Evolution of the Eastern Mediterranean Area, *Tectonophysics*, **60**, (1979), 1-42.

Lippmann, J., Stute, M., Torgersen, T., Moser, D., Hall, J., Lihung, L., Borcsik, M., Bellamy, R.E.S., and Onstott, T.C.: Dating Ultra-deep Mine Waters With Noble Gases and  ${}^{36}\text{Cl}$ , Witwatersrand Basin, South Africa, *Geochim. Cosmochim. Acta*, **67** (23), (2003), 4597-4619.

Lippmann, J.; Erzinger, J.; Zimmer, M.; Schloemer, S.; Eichinger, L.; and Faber, E.: On the Geochemistry of Gases and Noble Gas Isotopes (including  ${}^{222}\text{Rn}$ ) in Deep Crustal Fluids: the 4000 m KTB-Pilot Hole Fluid Production Test 2002-03, *Geofluids*, **5**, 1, (2005), 52-66.

Lupton, J.E.: Terrestrial Inert Gases: Isotope Tracer Studies and Clues to Primordial Components in the Mantle, *Annu. Rev. Earth Planetary Sci.*, **11**, (1983), 371-414.

Mc Kenzie, D.P.: Active Tectonics of the Mediterranean Region, *Geophys. J. R. Astron. Soc.*, **30**, (1972), 109-185.

Sano, Y., Takahata, N., Igarashi, G., Koizumi, N., and Sturchio, N.C.: Helium Degassing Related to the Kobe earthquake, *Chemical Geology*, **150**, (1998), 171-179.

Spakman, W.: Tomographic Mapping of the Upper Mantle Structure Beneath the Alpine Collision Belt. In Crust-Mantle Recycling at ConvergenceZones, S.R. Hart and L. Gülen (eds.), NATO ASI Series, C258, Kluwer Academic Publ., Dordrecht, (1989), 163-172.

Sugisaki R.: Changing  $\text{He}/\text{Ar}$  and  $\text{N}_2/\text{Ar}$  Ratio of Fault Air may be Earthquake Precursors, *Nature*, **275**, (1978), 209-211.

Şimşek, S.: Geothermal Model of Denizli, Sarayköy-Buldan Area, *Geothermics*, **14**, (1985), 393-417.

Şimşek, Ş.: Denizli, Kizildere, Tekkehama, Tosunlar, Buldan ve Yenice Alanları Jeolojisi ve Jeotermal Enerji Olanakları, MTA Report No 7486, (1984), Ankara.

Thomas, D.: Geochemical Precursors of Seismic Activity, *PAGEOPH*, **126**, Nos. 2-4, (1988), 239-266.

Toutain, J.P., and Baubron, J.C.: Gas Geochemistry and Seismotectonics: A Review, *Tectonophysics*, **304**, (1999), 1- 27.

Wiersberg, T., and Erzinger, J.: A helium Isotope Cross-section Study Through the San Andreas Fault at Seismogenic Depths, *Geochemistry Geophysics Geosystems (G3)*, 8, Q01002. (2007)